DEVELOPMENT OF SCANNING SYSTEM AT HIMAC

T. Furukawa #, T. Inaniwa, S. Sato, N. Saotome, Y. Takei, Y. Iwata, A. Nagano, S. Mori, S. Minohara, T. Shirai, T. Murakami, E. Takada, K. Noda and T. Kanai
National Institute of Radiological Sciences, Chiba, JAPAN

Abstract

A new treatment facility project, which will be an extension of the existing HIMAC complex, has been initiated for the further development of carbon-ion therapy. This new treatment facility will be equipped with a 3D irradiation system with pencil beam scanning. The most important criterion for the design study is how to realize the moving target irradiation by the scanning irradiation. For this purpose, we have studied a combination of the rescanning technique and the gated irradiation method based on fast scanning strategy. The design and the related study of the scanning system for the new HIMAC treatment facility are presented below.

INTRODUCTION

Heavy-ion beams such as carbon ion beams have attracted growing interest for cancer treatment due to their high dose localization and high biological effect at the Bragg peak. To make optimal use of these characteristics and achieve accurate treatment, 3D pencil beam scanning [1-3] is one of sophisticated techniques, and it has already been utilized for treatment at the PSI [2] and GSI [3]. At HIMAC, a project [4] to construct a new treatment facility was initiated for implementation of this irradiation technique in April 2006. The most challenging goal of this project is to realize treatment of a moving target by scanning irradiation [5], because pencil beam scanning is more sensitive to organ motions compared with the conventional broad-beam irradiation. To accomplish practical moving target irradiation, we decided to combine the rescanning technique and the gated irradiation method. Figure 1 shows the simulation result of dose distribution without/with rescanning and gating. For this purpose, we have studied 1) fast scanning, 2) moving target irradiation and 3) delivery verification system using a fluorescent screen and CCD camera. In this article, we describe the design and the experimental study of the verification.

STUDY OF FAST SCANNING

First task was to determine the best scanning method. To determine the most suitable scanning method for us, we needed to take the present status of HIMAC beam into account, because close cooperation with the beam control technique will bring it a feasible solution for the scanning strategy. Concerning the extraction status of the HIMAC synchrotron [6], we decided to employ the hybrid raster scanning method similar to GSI [3]. Furthermore, following developments are carried out toward fast scanning: 1) Treatment planning for fast scanning, 2) modification of synchrotron control, and 3) Fast scanning magnet. The technical details of them are referred to [5], [7] and [8]. Our goal is to achieve the irradiation time of moving target to be less than few minutes for 10 times rescanning with gating.

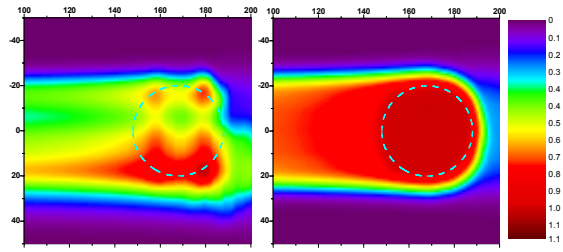

Figure 1: Simulation result of dose distribution of moving target irradiation without/with gating and rescanning.

In order to demonstrate the fast scanning (except fast scanning magnets), a scanning experiment with extended flattop of the HIMAC synchrotron was carried out, using the HIMAC scanning test course [9]. The irradiation control system was slightly modified so as to be capable of raster scanning irradiation instead of spot scanning irradiation. Figure 2 shows the oscilloscope display in this experiment. The dynamic intensity control system [6] controls the beam intensity almost constant during irradiation. In the experiment, the spherical target of 40 mm diameter was planned and irradiated. The total irradiation time was decreased to 20 s. The dose distributions measured by ionization chamber were in good agreement with the planned one at various penetration depths.

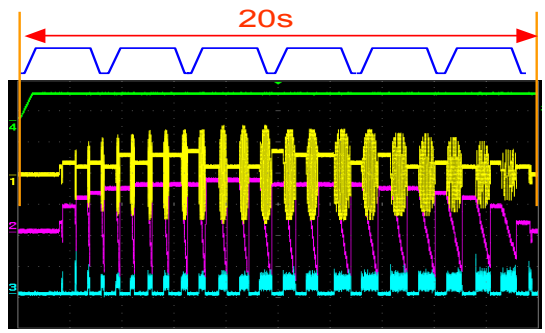

Figure 2: Oscilloscope display in the experiment. From the upper trace, the synchrotron excitation, the scanning magnet excitation current and the beam spill.

MOVING TARGET IRRADIATION

In the dynamic delivery such as scanning, the interplay effect between the beam motion and the target motion brings about hot and/or cold spots in the target volume. In

t_furu@nirs.go.jp

the rescanning method, regardless of the gating or non-gating, it is expected that the interplay effect statistically averaged the dose homogeneity in the target volume. However, the frequency and the phase correlation between the respiration motion and the scanning beam caused nonuniformity about dose distribution. Thus, it is necessary to adequately control the phase correlation with the limited number of rescans. Figure 3 shows the simulation result (non-gated) of dose distribution with uniform 2D scanning: (a) static plan, (b) deteriorated distribution by interplay and (c) expected dose distribution. By comparing Figs. 3 (b) and (c), one can see a significant difference between them. Thus, our interest is focused on how to obtain the statistically averaged distribution with the relatively smaller number of rescans. In this study, the scan speed and rescanning number dependence were studied by using simulation [10]. For the analysis of the delivered dose for the moving target, Bortfeld et al. [11] introduced the expected dose (i.e. Fig. 3 (c)), which is just a weighted average of the dose distribution without motion. As a result, we concluded that the total irradiation time needs to be integer times of the respiration cycle to obtain the averaging effect sufficiently. We named this the phase controlled rescanning (PCR) method [5,10]. Even in the slight difference between the respiratory cycle and the irradiation time, it is possible to obtain a dose distribution close to the expected one. This is a great advantage of the method, because the respiratory cycle is usually not constant during the irradiation.

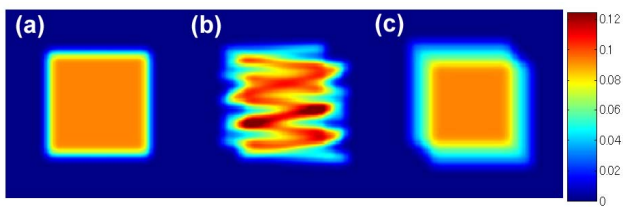

Figure 3: Simulation results of interplay effect in scanning irradiation; (a) static plan, (b) deteriorated distribution by interplay effect and (c) expected dose distribution.

The result mentioned above can be extended to 3D irradiation with gating. In the PCR method, it is necessary to adjust the irradiation time as the single respiration gate width. Owing to the extended flattop of the synchrotron and the flexibility of the beam intensity, it is possible to equalize the irradiation time of certain slice to the respiration gate width by adjusting the beam intensity slice-by-slice. Typical simulation results of 3D irradiation with and without the PCR method are compared in Fig. 4, which shows the percentage dose deviation from the expected one. In this simulation, the rescanning sequence was carried out only in the lateral xy plane, because the slowest direction of scanning was the beam depth axis of 200 ms compared with the magnetic scanning speed. As a result, it can be clearly seen that the PCR method makes it possible to realize the expected dose. In the rescanning without PCR, the field uniformity depends on the phase correlation between the respiration motion and the irradiation gate for each slice.

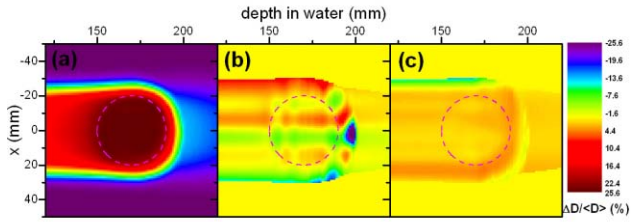

Figure 4: (a) Expected dose distribution in the xz plane and percentage dose deviations from expected one, (b) without and (c) with PCR in the case of 8 rescans.

Experimental studies are carried out at HIMAC. A 3D motion phantom was used in the rescanning experiment. This phantom consists of the xy stage and wedge for simulating 3D moving target. Owing to the high-power motor and its control unit, this system can operate not only the sinusoidal motion, but also arbitrary functions within the maximum speed and acceleration. Thus, it is possible to simulate realistic motion including the amplitude drift and the phase shift by using the patient data. In this stage, the fluorescent screen and CCD measurement system set on the xy stage are used for 2D dose deterioration measurement. Typical experimental results of 2D uniform scanning without gating are shown in Fig. 5. In this case, the sinusoidal motion was applied for the x direction. The simulation result is a close reproduction of the experimental result. Phase shift and amplitude drift in 3D irradiation will be studied in the future work.

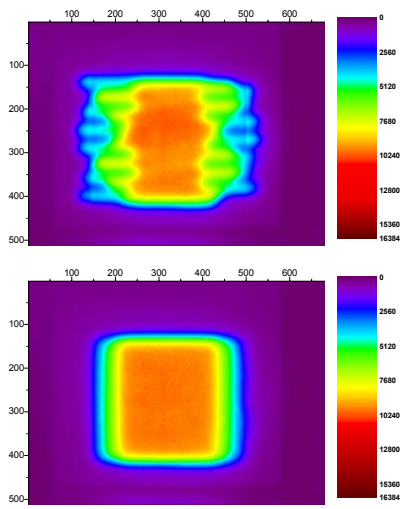

Figure 5: Measured 2D distribution without rescanning (left) and with 10 rescans and PCR method (right).

DELIVERY VERIFICATION SYSTEM

A quick verification of 3D dose distribution with the detector set in the beam line plays an important role not only in the verification of each irradiation but also in maintaining the irradiation record. For this purpose, we have developed a quick verification system by using a fluorescent screen with a CCD camera [12]. In this study,

the 3D dose distribution is reconstructed cooperating with the fluorescent screen measurement, in which slice-by-slice image acquisition and image intensity normalization by the count log of the main monitor play important roles. Since few assumptions are necessary in the reconstruction, it is simple and quite useful to directly compare the fluence distributions with the predicted one. However, the difference between them cannot derive the difference between the planned dose distribution and the delivered one. Thus, we focused on the reconstruction of the dose distribution.

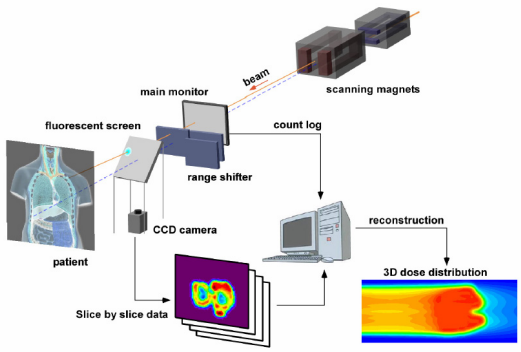

Figure 6: Schematic of the screen system layout.

For the experimental verification of this scheme, the beam study was carried out at HIMAC. In this verification, the reconstructed 3D dose distribution was compared with the ionization chamber measurement in the water phantom. The screen system was set at the final position of the experimental scanning port, as schematically shown in Fig. 6. The fluorescent screen, which is $Gd_2O_2S:Tb^{3+}$ on PET, was installed immediately downstream of the RSF. The screen was 320 μm thick. In this study, the PTV of an osteosarcoma patient treated at HIMAC was used as a clinical sample target, while irradiation parameters were optimized to obtain the uniform physical dose of 0.5 Gy by using the research version of the planning code [13]. Since this target was planned with 43 iso-energy slices, 43 images were obtained during the irradiation. Part of the measured images are shown in Fig 7. By applying the reconstruction calculation for these images, the 3D dose distribution can be obtained. Figure 8 shows the result of comparison between the ionization chamber measurement and the 3D dose reconstruction. It can be clearly seen that the reconstructed dose distribution is in good agreement with the measurement results of the ionization chamber. The slight difference between the planned and reconstructed dose distributions might be the result not only of delivery error, but also of measurement and reconstruction errors.

SUMMARY

The design and the related study of a 3D irradiation system with pencil beam scanning for the construction of a new treatment facility at HIMAC are well underway. This fast scanning was experimentally verified at HIMAC, except for the fast scanning magnet. For the moving target irradiation, the findings led us to draw the conclusion that the PCR method was a feasible solution. In this scheme, the dynamic beam-current control technique plays a key role. To ensure rapid verification of the beam delivery, we have developed a system using a fluorescent screen with CCD camera, and found it to be quite useful tool.

ACKNOWLEDGMENT

We would like to express our thanks to other members of Department of Accelerator and Medical Physics at NIRS for useful discussion. This work was carried out as a part of Research Project with Heavy Ions at NIRS-HIMAC.

REFERENCES

[1] T. Kanai et al, Nucl. Instr. Meth. 214 (1983) 491.
[2] E. Pedroni et al, Med. Phys. 22 (1995) 37.
[3] Th. Haberer et al, Nucl. Instr. Meth. A 330 (1993) 296.
[4] K. Noda et al, TUPP125, in these proceedings.
[5] T. Furukawa et al, Med. Phys. 34 (2007) 1085.
[6] T. Furukawa et al, Nucl. Instr. Meth. A560 (2006) 191.
[7] T. Inaniwa et al, Med. Phys. 34 (2007) 3302.
[8] Y. Iwata et al, TUPP118, in these proceedings.
[9] E. Urakabe et al, Jpn. J. Appl. Phys. 40 (2001) 2540.
[10] T. Furukawa et al, Proc. of NIRS-MD Anderson Symposium, NIRS-M-210 (2008).
[11] T. Bortfeld et al, Phys Med Biol. 2002;47(13):2203.
[12] T. Furukawa et al, Med. Phys. 35 (2008) 2235.
[13] T. Inaniwa et al, Nucl. Instr. Meth. B 266 (2008) 2194.

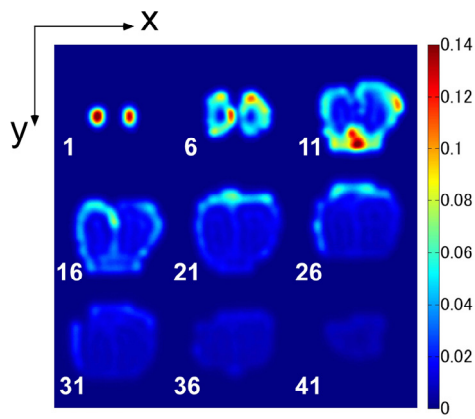

Figure 7: Part of the measured images. Scale of each image ranges from –50 to +50 mm in both the x and y directions.

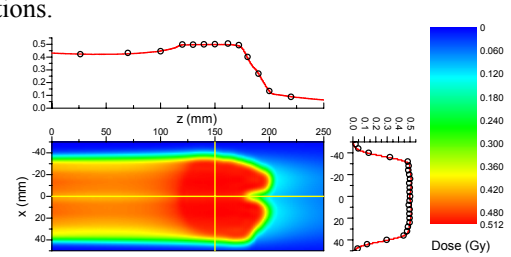

Figure 8: Comparison between the ionization chamber measurement (open circle) and the reconstructed dose distribution (center image and red line) in the xz plane.